

El Nino Induced Ocean Eddies in the Gulf of Alaska

**Arne Melsom, Harley E. Hurlburt, E. Joseph Metzger,
Steven D. Meyers and James J. O'Brien**

*Center for Ocean-Atmospheric Prediction Studies
The Florida State University
Tallahassee, FL 32306-3041*

*Submitted to Science
August, 1995*

Report 95-4

El Nino Induced Ocean Eddies in the Gulf of Alaska

Arne Melsom, Harley E. Hurlburt, E. Joseph Metzger, Steven D. Meyers
and James J. O'Brien*

1

Abstract

Observations reveal substantial eddy activity in the Gulf of Alaska, with the Sitka eddy being a frequently observed anticyclonic feature near 57°N. A unique high-resolution numerical model that accurately reproduces eddy formation, size, and lifetime is able to duplicate the observations. The decadal simulation allows examination of interannual variations in the eddy activity. Interannual variability in the upper ocean coastal circulation in the Gulf of Alaska is due to the El Nino/Southern Oscillation phenomenon in the tropical Pacific. El Nino events destabilize the Alaska Current, creating multiple strong anticyclonic eddies along the coast. These eddies then slowly propagate into the Gulf of Alaska and live for years. El Viejo (La Nina) events generally suppress eddy formation. This high latitude El Nino phenomena must have a major effect on local fisheries.

The continental slope of the northeast Pacific is a major habitat for a number of commercially harvested fish such as salmon, halibut and herring (1). It has been suggested that year-to-year changes in fish stock recruitment and return migration routes of certain species in the Gulf of Alaska are affected by low frequency ocean variability. A theory which has been advocated in several recent studies is that this variability may be attributed to El Nino/Southern Oscillation (ENSO) events which trigger propagating coastal Kelvin waves and also cause changes in the general atmospheric circulation (2, 3). A number of observational programs have been performed (4, 5), as well as several numerical model simulations (6, 7).

¹A. Melsom, Department of Geophysics, University of Oslo, P. O. Box 1022, Blindern, N-0315 Oslo, Norway.

H.E. Hurlburt and E.J. Metzger, Naval Research Laboratory, Stennis Space Center, MS, 39529-5004, USA.

S.D. Meyers and J.J. O'Brien, Center for Ocean-Atmospheric Prediction Studies, The Florida State University, Tallahassee, FL 32306-3041, USA.

High resolution numerical models of the ocean circulation allow study of mesoscale (~ 100 km) motion. Recent technological advances in computing have made it possible to apply these models to global and basin-scale domains. The effects of remote tropical events on mid-latitude mesoscale circulation through Kelvin wave teleconnections are now accurately represented. Moreover, the local response to the atmospheric circulation is well-described. These new high resolution global and basin-scale models realistically simulate the temporal and spatial variability of mesoscale circulation features. This class of numerical models is an important tool, since the limited quantity of *in situ* observations is a general, reoccurring problem for examination of ocean circulation on the mesoscale. Major features of the Navy Layered Ocean Model include isopycnal layers, nonlinear primitive equations, free surface and a semi-implicit time scheme (8,9,10).

We present results based on a simulation of the ocean circulation in the northern and tropical Pacific Ocean, from 20°S to 62°N . The model consists of six isopycnal layers and has a resolution of $1/8^{\circ} \times 45/256^{\circ}$ (latitude \times longitude) which is approximately 13 km in the Alaska Gyre region. The model was spun up to a statistical equilibrium using the Hellerman and Rosenstein (HR) monthly mean wind stress climatology (11). Subsequently, the model was forced for a 14 year period (1981-1994) starting January 1, 1981 with daily 1000 mb winds from the European Centre for Medium-Range Weather Forecasts (ECMWF) (10). The ECMWF 1981-1994 mean was replaced by the annual mean from HR. Previous numerical simulations of the Gulf of Alaska circulation used climatological or monthly winds, the present simulation incorporates a more accurate description of the temporal variability of the wind forcing.

We restrict our study to a subdomain in the eastern Gulf of Alaska bounded by 46°N to the south and 145°W to the west. We mostly discuss the results obtained for the two uppermost layers since these contain the essential dynamics of the upper ocean circulation.

The model accurately reproduces much of the observed variability in the region of interest, as illustrated by model comparisons with coastal stations. The results in Fig. 1 exemplify this good agreement and validates the numerical representation of the annual and interannual variability. The dominance of ENSO events in the interannual variability along the coast of the Gulf of Alaska is apparent in Fig. 1b. This variability has a strong effect on the local circulation.

A coastal current, corresponding to the Alaska Current, is observed in the simulation results. This current is strongest during winter, when the flow is northward. In spring the current weakens, moves slightly offshore, and breaks into eddies. During summer its direction is frequently southward. A similar seasonal cycle is found in observational data (12), where it is attributed to a shift in the atmospheric circulation from a surface pressure low in winter to a summer high (13). The transport and the vertical velocity shear associated with the coastal current reach maximum values in December or January. At this time, the current starts to meander. The alongshore wavelength and offshore amplitude of the meanders are typically 200 km and 40 km, respectively. However, the amplitude may become ~ 100 km, after which the current usually breaks into eddies. The meandering is observed in both of the layers under consideration. Generally, the horizontal pressure gradient is significantly larger in layer 1 than in layer 2. Hence, the motion in the meanders is strongly baroclinic and the accompanying vertical velocity shear is significant.

As the meanders break up, anticyclonic and cyclonic eddies are formed by baroclinic instability. The anticyclonic eddies are generally larger than the cyclonic eddies. The cyclonic eddies dissipate quite rapidly, whereas the anticyclonic eddies sometimes survive for well over a year. Typically, the stronger anticyclonic eddies are generated during winter. The eddies are seen to propagate slowly southwestward (i.e., offshore), with an estimated propagation speed of 0.5-1 cm/s, or 200 km/year. However, the direction of propagation may temporarily be reversed, possibly due to the local wind forcing.

Following conventional theory for baroclinic instability, the wavelength of the most rapidly growing disturbance is a function of the buoyancy, layer thickness and latitude (14). In the coastal regions of the Gulf of Alaska this scale varies from 50 km to 75 km for upwelling and downwelling perturbations, respectively. Thus, downwelling instabilities are well resolved, whereas the description of unstable disturbances in the upwelling situation is less precise.

Upwelling perturbations stabilize the flow and do not yield eddies. Additionally, the generation of cyclonic eddies may be artificially suppressed due to their relatively small horizontal extent, since horizontal gradients are dampened by a Laplacian friction which selectively dampens small scales. (This is necessary for numerical stability).

In an extensive examination of oceanographic data collected during 1927-77 in the Gulf of Alaska, Tabata (15) concluded that "baroclinic eddies occur frequently in this region. Among these is the recurring, well developed, anticyclonic eddy situated within a few hundred kilometers of Sitka", now commonly called the Sitka eddy (13).

The diameter of the Sitka eddy is observed to be 200 km - 300 km, with a vertical isopycnal deflection of 20 m - 100 m. Furthermore, the initial location of the Sitka eddy is 150 km - 200 km off the coast of Baranof Island, and it can persist for 10 to 17 months, drifting southwestward. All of these aspects of the Sitka eddy are reproduced qualitatively and quantitatively by the numerical model (diameter 150 km - 300 km, isopycnal deflection of up to 100 m, initial location 200 km off Baranof Is., persisting for longer than one year).

Tabata (15) indicates that one or more anticyclonic eddies exist off Sitka during most years, if not every year. A Sitka eddy was definitely present in 1958, 1960, 1961 and 1977. The data also give some evidence of the Sitka eddy in 1954, 1956, 1959, 1962 and 1967. For many years the data are insufficient to draw any conclusion. The numerical model produces at least one anticyclonic eddy off Sitka in six of the nine eddy generation seasons. In 1984, the circulation in the region is dominated by the lasting effect of the strong eddy that was generated the year before; and although the isopycnal interfaces do not clearly indicate the presence of an eddy in the winter and spring of 1985, the circulation in the region is distinctly anticyclonic. The 1989 season follows an El Viejo event and eddies are not generated. (El Viejo means cold SST anomalies in the tropical Pacific and is the opposite phase from El Nino.)

During the model run, there are several years that are classified as El Nino years in the tropical Pacific. The largest El Nino event in recent history occurred during the 1982/83 boreal (northern) winter. Between 1981 and 1991 there is only one recognized El Viejo event - during the 1988/89 boreal winter.

Figure 2 shows the deflection of the interface between the second and third layer in the model during an El Nino and an El Viejo. This depiction indicates an ENSO influence on eddy generation in the Gulf of Alaska. Furthermore, keeping in mind that the mean depth of the upper two layers is ~ 170 m in coastal regions, the ENSO effect is substantial in this area. Extreme events in the tropical Pacific Ocean affects both the atmospheric and oceanic

circulation. It is impossible to conclude from Fig. 2 alone whether the changes that are seen in the area are due to remote forcing in the ocean through a coastal Kelvin wave teleconnection (16) or due to changes in the local atmospheric forcing. Both forcings are present in the model dynamics and it is difficult to separate their independent effects. However, coastal Kelvin waves are clearly observed in the model to propagate from the equatorial Pacific into the Gulf of Alaska. Their arrival in the Gulf is immediately antecedent to the disruption of the Alaska Current and the formation of eddies.

Previous studies have hypothesized that the interannual variability in the Gulf of Alaska may be affected by ENSO events in the tropical Pacific Ocean (2, 3). Although such a link is not discussed by Tabata, the observations of the Sitka eddy indicate interannual variability, yielding clues to any relationship with the tropical ocean. In his study, Tabata refers to the possible presence of the Sitka eddy with various degrees of certainty (“a hint of it”, “a suggestion of it”, “definite indication” and so on). Though the various degrees of certainty in the observational information may be attributed to the sparsity of available data, it is likely this reflects the interannual variability of the mesoscale ocean circulation off Sitka as well. If the Sitka eddy is weak, it will be correspondingly hard to detect in the observational data. As can be seen from Fig. 3, the simulation results contain a significant amount of mesoscale variability in this region.

In the datasets that are surveyed by Tabata (15), the spring of 1958, the summers of 1960 and 1961, and the spring of 1977 are the times when the Sitka eddy was undoubtedly present. Both 1957/58 and 1976/77 were seasons with an El Nino event in the tropical Pacific Ocean. This corresponds well to the results of the numerical simulation: the 1982/83 El Nino was the largest in the 20th century and appears to have produced eddies in the Gulf of Alaska. On the other hand, the 1986/87 El Nino, which was of moderate size, does not spawn a large number of eddies in the Gulf of Alaska in the numerical model, so the evidence is inconclusive. The lack of a significant ENSO response in 1986/87 may be due to inadequate ECMWF winds over the equatorial Pacific during this time.

Repression of eddy activity following El Viejo tropical events is supported by the measurements off Sitka. There are two such events reviewed in Tabata (15), which occur in 1955/56 and 1956/57 El Viejo events. In the spring and summer of 1956 and 1957, Tabata concludes that the Sitka eddy is either

weak or non-existent. Following the 1988/89 El Viejo tropical event, the eddy activity in the Gulf of Alaska is strongly suppressed in the numerical model.

Both the observational data and the model result suggest that the interannual variability in the Gulf of Alaska is correlated with El Nino and El Viejo events in the tropical Pacific Ocean. The long-term effect of such events in the North Pacific Ocean circulation was recently reported based on results from another version of the present numerical model (17). There it was demonstrated that the 1982/83 El Nino triggered planetary waves that crossed the North Pacific basin and caused a partial northward re-routing of the Kuroshio Extension in 1992-93. This paper demonstrates that the high-latitude ocean also responds strongly to ENSO events, having memory over thousands of kilometers and many years. The discovery of remotely forced interannual changes in upper ocean circulation heralds a new era in understanding the behavior of the upper ocean on short-term climate scales. How these oceanic changes effect marine life or local weather patterns is not fully understood.

REFERENCES

1. R. K. Reed, R. D. Muench, J. D. Schumacher, *Deep-Sea Res.* **27**, 509 (1980).
2. R. K. Reed, *Deep-Sea Res.* **31**, 169 (1984).
3. P. F. Cummins, *J. Phys. Oceanogr.* **19**, 1649 (1989).
4. P. K. Heim, M. A. Johnson, J. J. O'Brien, *J. Geophys. Res.* **97C**, 17,765 (1992).
5. P. F. Cummins and L. A. Mysak, *J. Phys. Oceanogr.* **18**, 1261 (1988).
6. W. J. Emery and K. Hamilton, *J. Geophys. Res.* **90C**, 857 (1985).
7. L. A. Mysak, in *El Nino north: Nino effects in the eastern subarctic Pacific Ocean*, W. S. Wooster, Ed. (Univ. of Washington Sea Grant Publ., 1985) p. 97.
8. H.E. Hurlburt and J.O. Thompson, *J. Phys. Oceanogr.* **10**, 1611, (1980).
9. A. J. Wallcraft, NOARL Report no 35, Naval Res. Lab., Stennis Space Center, MS, 21 pp (1991).
10. H.E. Hurlburt, A.J. Wallcraft, W.J. Schmitz, Jr., P.J. Hogan and E.J. Metzger, *J. Geophys. Res.*, (in press), (1995).
11. S. Hellerman and M. Rosenstein, *J. Phys. Oceanogr.* **13**, 1093 (1983).

12. G. S. E. Lagerloef, R. D. Muench, J. D. Schumacher, *J. Phys. Oceanogr.* **11**, 627 (1981).
13. T. C. Royer, *Deep Sea Res.* **22**, 403 (1975).
14. E. A. Eady, *Tellus* **1**, 33 (1949).
15. S. Tabata, *J. Phys. Oceanogr.*, **12**, 1260 (1982).
16. D.B. Chelton and R.E. Davis, *J. Phys. Oceanogr.*, **12**, 757 (1982).
17. G. A. Jacobs, H. E. Hurlburt, J. C. Kindle, E. J. Metzger, J. L. Mitchell, W. J. Teague, A. J. Wallcraft, *Nature*, **370**, 360 (1994).
18. Financial supported is provided by SERDP and by the Norwegian Science Council (Norges Forskningsrad). The Physical Oceanography Branch of the Office of Naval Research provides the base support for Center for Ocean-Atmosphere Prediction Studies. Thanks for D. Muller for many helpful discussions.

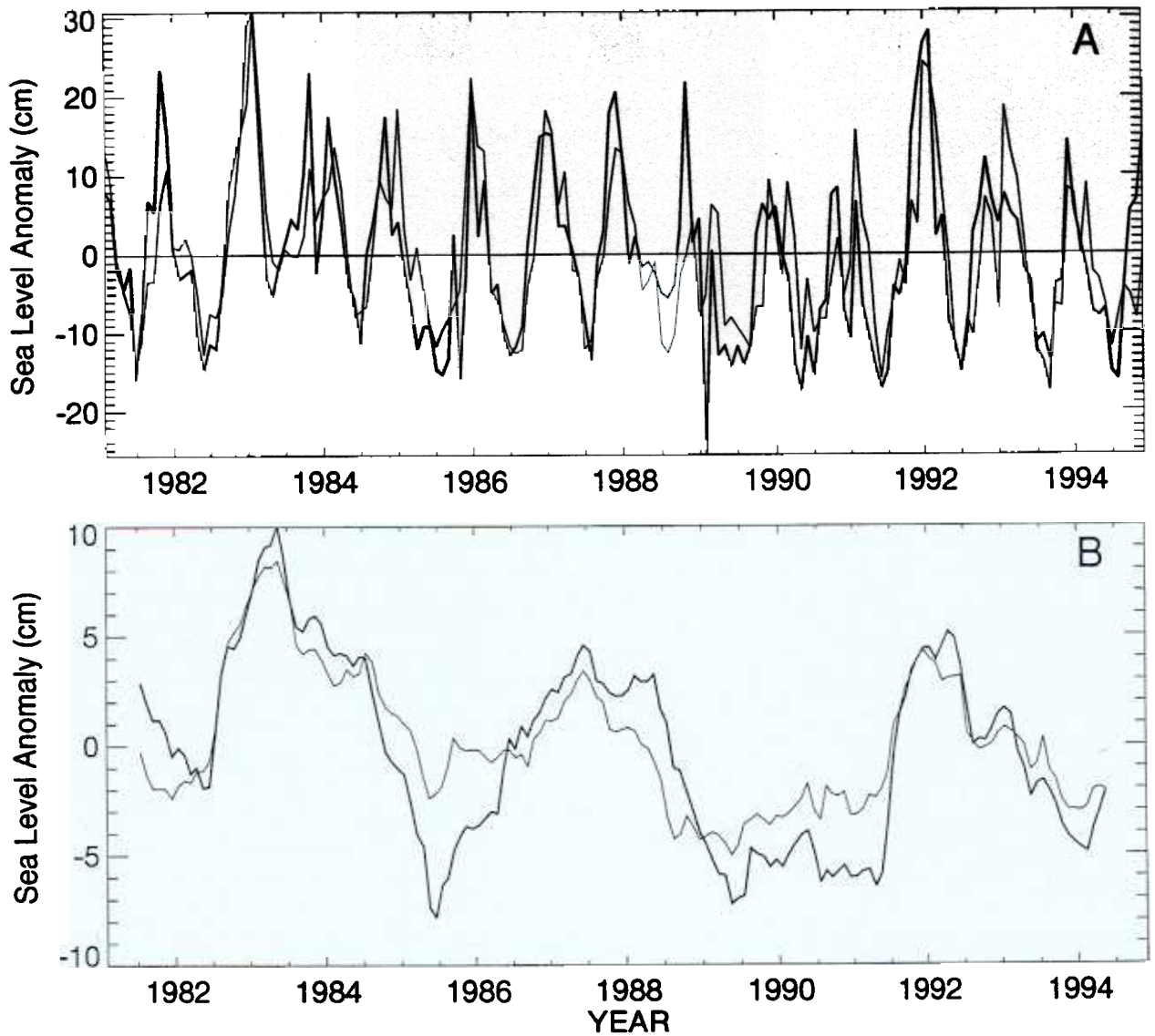
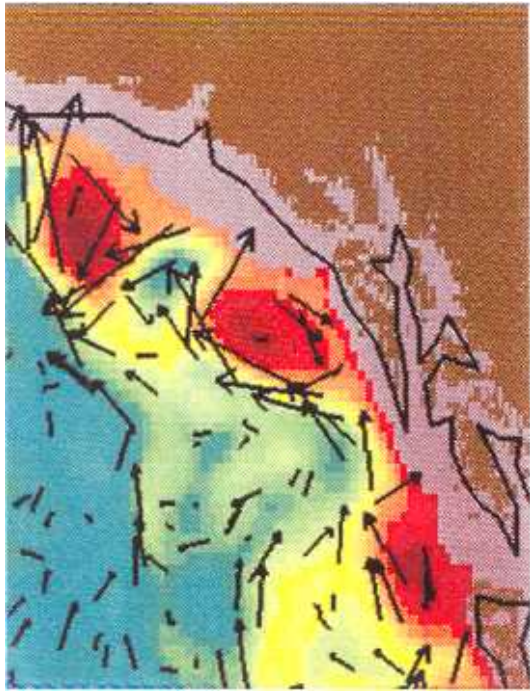


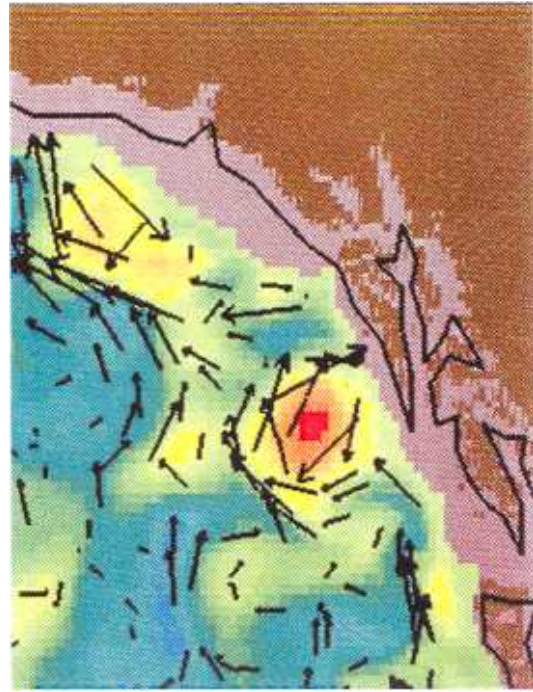
Figure 1: A comparison of sea level observed at Sitka, Alaska with sea level in the ocean model. Thick line is from the IGOSS station at Sitka, AK. Thin line is model results. (A) Anomaly of absolute sea level. (B) After removal of the annual sinusoid obtained through a least-squares fit. The anomaly was filtered with a one year boxcar filter.

Figure 2: ENSO signal in the Gulf of Alaska from the simulation. The ocean circulation in the Gulf of Alaska following the 1982/83 El Nino in the tropical Pacific Ocean is shown on the left-hand side. The situation following the 1988/89 El Viejo event (La Nina) is displayed to the right. Both depictions show the situation on February 13 (1983 and 1989). The colors indicate the deviation of the thickness of the two upper layers from the seasonal mean. Yellow and red colors show downwelled regions; blue and purple colors correspond to upwelled; and green colors indicate values close to the mean. The arrows depict the direction and strength of the currents.

Figure 3: Interannual mesoscale variability. The ocean circulation that results from the numerical simulation is depicted for the same day (February 28) of 4 different years. Here, (a), (b), (c) and (d) correspond to 1983, 1986, 1988 and 1989, respectively. Note that (a) and (c) follow El Nino events in the tropical Pacific Ocean, whereas (d) follows a El Viejo event. The anticyclonic circulation that is observed in (d) is a remnant of the eddies that were generated the year before. The color coding is the same as in Figure 2.



a



b



c



d

